

Linear and Nonlinear Chip-Rate Minimum Mean-Squared-Error Multiuser CDMA Detection

Yao Ma, *Member, IEEE*, and Teng Joon Lim, *Member, IEEE*

Abstract—In this paper, a linear Kalman filter detector for code-division multiple access proposed earlier in the literature is extended to a structure that can handle arbitrary detection delays, through the mechanism of state augmentation. Because pre-detection RAKE combining is used in the detector, it is optimal for multipath channels, unlike the previous structure that performed post-detection combining. We also derive nonlinear Kalman detectors, which approximate the highly complex nonlinear minimum mean-squared-error detector, using the concept of “additional observations.” Both linear and nonlinear detectors require processing at one or more times the chip rate, and knowledge of the spreading codes of interfering users. They have the advantage over many other multiuser detection algorithms of not requiring the spreading codes to be periodic at the symbol rate, or matrix inversion. In addition, two of the detectors are able to generate and update *a posteriori* probabilities of the transmitted symbols, making them interesting for iterative multiuser detection.

Index Terms—Code-division multiple access, Kalman filtering, minimum mean-squared-error detection, multiuser channels.

I. INTRODUCTION

IN A multiuser code-division multiple-access (CDMA) communication link, multiple users transmit simultaneously over the same frequency band using spread-spectrum signals and different spreading codes. Due to multipath propagation and asynchronism in the signals received from different users, multiple-access interference (MAI) exists irrespective of code design, and limits system performance. Multiuser detection [1] is the generic name for a class of detection techniques designed to combat MAI and hence improve performance. In this work, we are interested in linear [2] and nonlinear minimum mean-squared-error (MMSE) multiuser detectors.

Linear MMSE (LMMSE) detectors may be implemented using symbol-rate adaptive algorithms [3], [4] in short-code systems, with or without training sequences. For long-code systems, a sampling-rate Kalman detector has been proposed [5] to implement the LMMSE detector without matrix inversions or training sequences in frequency-selective asynchronous channels when the spreading codes for all users are assumed known. Prior to that work, Chen and Roy [6] devised a sampling-rate

recursive least squares (RLS) detector which converged to the decorrelating detector in synchronous channels under the same assumption.

In this paper, we relax the zero detection delay constraint¹ in [5] and point out that with multipath channels, the optimal detector structure combines the multipaths before MMSE detection (pre-detection combining). This was mentioned briefly in [7], but not in [5], which treated each path separately and then coherently combined the multipath signals to make a decision. The latter structure also has a higher computational complexity. Here we develop the pre-detection RAKE combining algorithm fully.

We further observe that the linear state-space model used to develop the Kalman filter algorithm is non-Gaussian because of the discrete nature of the channel inputs, which appear in the “state noise” term, and so the linear Kalman detector does not yield conditional mean (CM) estimates. We therefore derive a recursive algorithm for computing the optimal, nonlinear MMSE (or CM) detector based on the exact probability density function (pdf) of the state noise, and propose two simpler but suboptimal nonlinear Kalman detectors that use the concept of “additional observations,” as introduced by Thielecke in [8] and [9]. The soft-decision (SD) and hard-decision (HD) detectors introduce one or more additional stages of processing at each user’s symbol boundary, based on feeding back soft or hard decisions, respectively.

The performance of the new algorithms are evaluated using both a semianalytical technique and simulations, and the nonlinear algorithms are seen to have a distinct advantage over the linear ones especially in additive white Gaussian noise (AWGN) channels. Finally, the computational complexity for each of the algorithms in terms of the number of multiplications per detected symbol is derived. It is shown that the complexity of the algorithms is of the order of K^2 , where K is the number of users.

II. SYSTEM MODELS AND LINEAR KALMAN DETECTION

A. Pathwise Model

It is assumed that K users simultaneously transmit over independent multipath fading channels with L resolvable paths each. After chip-matched filtering and sampling at a rate at least equal to the chip rate, the baseband received signal is given by

$$y(n) = \sum_{k=1}^K \sum_{l=1}^L c_{kl}(n) d_k(i_{kl}) s_k(n - \tau_{kl}) + v(n) \quad (1)$$

¹Larger delays improve performance in asynchronous channels and dispersive channels.

Paper approved by R. Kohno, the Editor for Spread-Spectrum Theory and Applications of the IEEE Communications Society. Manuscript received January 5, 2000; revised May 1, 2000.

Y. Ma is with the Centre for Wireless Communications, Singapore 117674, Singapore (e-mail: mayao@cw.cw.nus.edu.sg).

T. J. Lim was with the Centre for Wireless Communications, Singapore 117674, Singapore. He is now with the Department of Electrical and Computer Engineering, University of Toronto, Toronto, ON M5S 3G4, Canada (e-mail: limtj@comm.toronto.edu).

Publisher Item Identifier S 0090-6778(01)02181-X.

where $c_{kl}(n)$ is the complex attenuation for the l th path of the k th user, $d_k(i)$ is the i th symbol transmitted by the k th user, τ_{kl} is the time delay introduced by the l th path of the k th user (quantized to the nearest sample), $v(n)$ is additive white Gaussian noise of variance σ^2 , $s_k(n)$ is the k th user's spreading sequence, and $i_{kl} = \lfloor (n - \tau_{kl})/T \rfloor$ is the symbol index for the symbol received from the k th user over the l th path at time n . Finally, T is the number of samples in a symbol period.

For the state-space model proposed in [5], the observation equation is given by

$$y(n) = \mathbf{h}_{1,n}^\top \mathbf{x}(n) + v(n) \quad (2)$$

where $\mathbf{x}(n) = [c_{11}d_1(i_{11}), c_{12}d_1(i_{12}), \dots, c_{KL}d_K(i_{KL})]^\top \in \mathbb{C}^{KL \times 1}$ is the state vector at sampling instant n , and $\mathbf{h}_{1,n}^\top = [s_1(n - \tau_{11}), s_1(n - \tau_{12}), \dots, s_K(n - \tau_{KL})]$. The state transition equation is given by

$$\mathbf{x}(n) = \Phi_n \mathbf{x}(n-1) + \mathbf{w}(n) \quad (3)$$

where

$$\Phi_n = \begin{cases} \mathbf{I}, & n \neq iT + \tau_{kl} \\ \text{diag}(\underbrace{1, \dots, 1}_{(k-1)L+l-1}, 0, \underbrace{1, \dots, 1}_{(K-k+1)L-l}), & n = iT + \tau_{kl} \end{cases}$$

$\mathbf{w}(n)$ is the state noise vector and its covariance matrix is given by

$$\mathbf{Q}_n = \begin{cases} \mathbf{0}, & n \neq iT + \tau_{kl} \\ \text{diag}(\underbrace{0, \dots, 0}_{(k-1)L+l-1}, 1, \underbrace{0, \dots, 0}_{(K-k+1)L-l}), & n = iT + \tau_{kl}. \end{cases}$$

In this state-space model, every path of every user is treated as a virtual user. The detector estimates the signals $c_{kl}d_k(i_{kl})$, and then coherently combines the L estimates belonging to a desired user to form a symbol estimate. This structure is not optimal² and detector performance will degrade quickly as KL becomes large with respect to the spreading gain. Furthermore, the computational complexity is proportional to L^2 . Another shortcoming of the detector is that a desired symbol must be detected without delay, whereas we know that in asynchronous systems, detector performance improves as detection delay increases.

B. Combined-Multipath Model

It is pointed out in [10] and [11] that the multipath combining decorrelating (mD) detector, which does multipath combining before decorrelating detection, is optimally near-far resistant for multipath fading channels, and performs uniformly better than the decorrelating multipath combining (Dm) detector, which performs post-detection combining. Since the linear MMSE detector converges to the decorrelating detector at high signal-to-noise ratios, it can be concluded that the pre-detection combining MMSE detector to be discussed presently performs better than the post-detection combining MMSE detector of [5]. This observation is verified later by simulation results.

In [11], a symbol-synchronous multipath channel is considered and the detector processes the received signal at the symbol rate. We will consider a more general channel model where the

²Because it uses up KL degrees of freedom when only K users are desired.

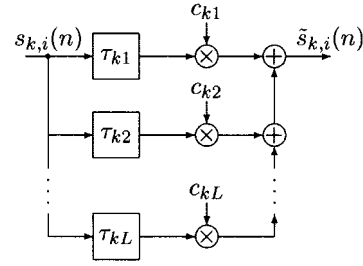


Fig. 1. Generating the channel-distorted or received spreading code $\tilde{s}_k(n)$ from the transmitted spreading code $s_k(n)$. $s_{k,i}(n) = s_k(n)u_T(n-iT)$ is the T -sample window of the spreading code that modulates $d_k(i)$ at the transmitter.

symbol timing of the users may be different and the multipath delay spreads may be arbitrarily large, thereby accommodating severe intersymbol interference.

We now describe a state-space model in which the channel-distorted spreading codes are used as inputs to the Kalman filter, which consequently estimates only K parameters and is less complex than the one described in [5].

The received signal is now expressed as

$$y(n) = \sum_{i=0}^{\infty} \sum_{k=1}^K d_k(i) \tilde{s}_{k,i}(n) + v(n) \quad (4)$$

where

$$\tilde{s}_{k,i}(n) = \sum_{l=1}^L c_{kl}(n) s_k(n - \tau_{kl}) u_T(n - iT - \tau_{kl})$$

is the “received” spreading code modulating $d_k(i)$, and may be generated at the receiver by the filter shown in Fig. 1; $u_T(n) = \begin{cases} 1 & 0 \leq n < T \\ 0 & \text{otherwise} \end{cases}$ is a unit rectangular pulse of width T samples.

Clearly, the first term on the right-hand side (RHS) of (4) can be written as a vector inner product so that

$$y(n) = \mathbf{h}_n^\top \mathbf{d}(n) + v(n) \quad (5)$$

where $\mathbf{d}(n)$ is a “state vector” containing (but not limited to) all the symbols contributing to $y(n)$, and $\mathbf{h}(n)$ is the measurement matrix containing samples of $\tilde{s}_k(n)$, $k = 1, \dots, K$. Unlike the model of [5], we allow for arbitrary detection delays by deliberately having symbols not directly affecting $y(n)$ in $\mathbf{d}(n)$. Specifically, we can define

$$\mathbf{d}(n) = \begin{bmatrix} \mathbf{d}_0(n) \\ \mathbf{d}_1(n) \\ \vdots \\ \mathbf{d}_{N_d}(n) \end{bmatrix} \in \mathbb{C}^{(N_d+1)K \times 1} \quad (6)$$

where $\mathbf{d}_q(n) = [d_1(i_{11} - q), \dots, d_K(i_{K1} - q)]^\top$, $q = 0, \dots, N_d$, and N_d can be regarded as the detection delay measured in number of symbol intervals. The elements of $\mathbf{d}(n)$ that do not directly affect $y(n)$ will be taken care of by zeros in the matching positions of \mathbf{h}_n . To simplify notation, we observe that in the combined-multipath model, the subscript l is no longer needed since the individual paths are all absorbed into one channel-distorted spreading code. Therefore, we will drop the subscript l and write τ_k for τ_{k1} and i_k for i_{k1} from here on.

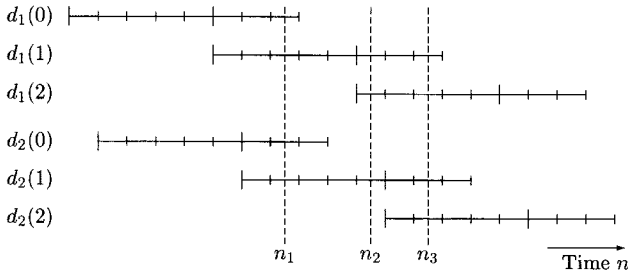


Fig. 2. Two-user example, with the interval between small ticks = $0.2T$ and the big ticks representing symbol boundaries.

Given knowledge of $\tilde{s}_k(n)$ for $k = 1, \dots, K$, \mathbf{h}_n is known and (5) may thus be used as the observation equation in a Kalman filter. We now require a state transition equation which describes the time variation of $\mathbf{d}(n)$. It is important to note that the symbol indices i_k are functions of n and τ_k . Equally important is the fact that when $\tau_j \neq \tau_k$ for some j and k , i_j and i_k are incremented at different time instants. The consequences of these two observations will now be explained with a two-user example, and then generalized.

Assume that $\tau_1 = 0$ (this can be assumed for all systems without loss of generality) and $\tau_2 = 0.2T$, and that the delay spreads are 0.6 symbol intervals for both users. The lines in Fig. 2 represent the nonzero signal contributions of the six symbols $d_1(0), d_1(1), d_1(2), d_2(0), d_2(1), d_2(2)$ to the received signal. Supposing that $N_d = 1$,³ we have

$$\begin{aligned} \mathbf{d}(n_1) &= [d_1(1), d_2(1), d_1(0), d_2(0)]^T \\ \mathbf{d}(n_2) &= [d_1(2), d_2(1), d_1(1), d_2(0)]^T \\ \mathbf{d}(n_3) &= [d_1(2), d_2(2), d_1(1), d_2(1)]^T. \end{aligned}$$

The following points should be noted.

- 1) When $n = n_2$, even though $d_2(0)$ is no longer affecting the received signal, we still keep it in the state vector $\mathbf{d}(n)$ in order to keep the dimension of the state vector constant over time.
- 2) The symbol index for user 1 changes at a different time from user 2.
- 3) When i_1 is incremented, the entries of $\mathbf{d}(n)$ belonging to the first user effectively leap-frogs over those of the second user, and the new symbol $d_1(i_1)$ is shifted into the first position of $\mathbf{d}(n)$.

For a K -user system, the last point translates into the user whose symbol index is incremented leap-frogging over the other $K - 1$ users, and having one new symbol shifted into the state vector and one old one shifted out. This behavior is succinctly captured by the state transition equation

$$\mathbf{d}(n) = \Phi_n \mathbf{d}(n-1) + \mathbf{w}(n) \quad (7)$$

³Note that this is the minimum value of N_d in this case. Choosing $N_d = 0$ will result in some of the signal energy being ignored, and hence worse performance. In general, the minimum value of N_d is $\max_k [\Delta\tau_k/T_s]$, where $\Delta\tau_k$ is the channel delay spread of the k th user and T_s is the symbol interval.

where for any $i \in \mathbb{Z}$ and any $k \in \{1, 2, \dots, K\}$

$$\Phi_n = \begin{cases} \mathbf{I}, & n \neq iT + \tau_k \\ \mathbf{E}_k, & n = iT + \tau_k \end{cases} \quad (8)$$

$$\mathbf{w}(n) = \begin{cases} \mathbf{0}, & n \neq iT + \tau_k \\ [\mathbf{0}_{k-1}, d_k(i), \mathbf{0}_{(N_d+1)K-k}]^T, & n = iT + \tau_k \end{cases} \quad (9)$$

$$\begin{aligned} \mathbf{Q}_n &= \mathbf{E}[\mathbf{w}(n)\mathbf{w}(n)] \\ &= \begin{cases} \mathbf{0}, & n \neq iT + \tau_k \\ \text{diag}(\mathbf{0}_{k-1}^T, 1, \mathbf{0}_{(N_d+1)K-k}^T), & n = iT + \tau_k \end{cases} \end{aligned} \quad (10)$$

and $d_k(i) \in \{e^{j2\pi(m-1)/M}\}_{m=1, \dots, M}$ is the new symbol shifted in at the symbol boundary. The matrix $\mathbf{E}_k \in (0, 1)^{(N_d+1)K \times (N_d+1)K}$ in (8) is obtained from the identity matrix \mathbf{I} by shifting the elements of the $(lK + k)$ th, $l = 0, \dots, N_d$, column downwards by K places.

With (7) and (5), we now have an exact state-space model for the multiuser CDMA system, which we will use to develop linear and nonlinear Kalman detectors.

C. Linear Kalman Detector

The Kalman filter updates the error covariance matrices \mathbf{P}_n^- and \mathbf{P}_n^+ according to the following equations [12]:

$$\mathbf{P}_n^- = \Phi_n \mathbf{P}_{n-1}^+ \Phi_n^T + \mathbf{Q}_n \quad (11)$$

$$\mathbf{k}_n = \mathbf{P}_n^- \mathbf{h}_n (\mathbf{h}_n^T \mathbf{P}_n^- \mathbf{h}_n + \sigma^2)^{-1} \quad (12)$$

$$\mathbf{P}_n^+ = (\mathbf{I} - \mathbf{k}_n \mathbf{h}_n^T) \mathbf{P}_n^- \quad (13)$$

Estimates of the state vector $\mathbf{d}(n)$ are obtained recursively as

$$\hat{\mathbf{d}}(n) = \phi_n \hat{\mathbf{d}}(n-1) + \mathbf{k}_n [y(n) - \mathbf{h}_n^T \Phi_n \hat{\mathbf{d}}(n-1)] \quad (14)$$

where $\hat{\mathbf{d}}(n)$ is the filtered state estimate at instant n , and $\Phi_n \hat{\mathbf{d}}(n-1)$ is the corresponding predicted state estimate. When both state and observation noise processes are Gaussian, $\hat{\mathbf{d}}(n) = E[\mathbf{d}(n) | \mathcal{Y}_n]$ and $\Phi_n \hat{\mathbf{d}}(n-1) = E[\mathbf{d}(n) | \mathcal{Y}_{n-1}]$. \mathcal{Y}_n denotes the set of observations up to and including the n th sampling interval. If we define $\mathbf{e}(n) = \mathbf{d}(n) - \Phi_n \hat{\mathbf{d}}(n-1)$ and $\varepsilon(n) = \mathbf{d}(n) - \hat{\mathbf{d}}(n)$ as the predicted and filtered state error vectors, respectively, then in (11)–(13), $\mathbf{P}_n^- = E(\mathbf{e}(n)\mathbf{e}^H(n))$ and $\mathbf{P}_n^+ = E(\varepsilon(n)\varepsilon^H(n))$ are the predicted and filtered state error covariance matrices, respectively, and \mathbf{k}_n is the Kalman gain vector.

At symbol boundaries for user k , i.e., when $n = iT + \tau_k$, we extract $\hat{\mathbf{d}}_k(i - N_d)$ from $\hat{\mathbf{d}}(n)$, which is the smoothed soft estimate of the symbol $d_k(i - N_d)$. A final hard decision is then obtained using a memoryless slicer.

III. NONLINEAR DETECTORS

A. Recursive Nonlinear MMSE Detector

The linear Kalman detector discussed in the previous section will provide optimal MMSE⁴ performance if both the state noise

⁴This term is used interchangeably with “conditional mean” because it is well known (see, e.g., [13]) that MMSE (usually nonlinear) and CM estimates are identical.

and the observation noise are Gaussian. However, this condition is not satisfied since the nonzero element $d_k(i)$ in the state noise vector $\mathbf{w}(n)$ at the symbol boundaries is a discrete random variable. Therefore, the Kalman detector provides only linear MMSE detection performance. In this section, we will derive a recursive algorithm for finding the optimal MMSE detector using Bayes' rule.

The optimal MMSE state estimate is given by the conditional mean $E[\mathbf{d}(n) | \mathcal{Y}_n]$, which requires $P[\mathbf{d}(n) | \mathcal{Y}_n]$, the probability of $\mathbf{d}(n)$ conditioned on \mathcal{Y}_n . Using Bayes' rule we can compute $P[\mathbf{d}(n) | \mathcal{Y}_n]$ recursively in time by

$$P[\mathbf{d}(n) | \mathcal{Y}_{n-1}] = \sum_{\mathbf{d}(n-1)} P[\mathbf{d}(n-1) | \mathcal{Y}_{n-1}] P[\mathbf{d}(n) | \mathbf{d}(n-1)] \quad (15)$$

$$P[\mathbf{d}(n) | \mathcal{Y}_n] = \frac{p[y(n) | \mathbf{d}(n)] P[\mathbf{d}(n) | \mathcal{Y}_{n-1}]}{p[y(n) | \mathcal{Y}_{n-1}]} \quad (16)$$

It is to be noted that for discrete random variables, we use probability mass functions (pmfs) $P(\cdot)$ and for continuous random variables we use pdfs $p(\cdot)$.

This iterative algorithm to derive $P[\mathbf{d}(n) | \mathcal{Y}_n]$ from $P[\mathbf{d}(n-1) | \mathcal{Y}_{n-1}]$ can be computed only if the conditional probability functions $P[\mathbf{d}(n) | \mathbf{d}(n-1)]$, $p[y(n) | \mathbf{d}(n)]$, $P[\mathbf{d}(n) | \mathcal{Y}_{n-1}]$ and $p[y(n) | \mathcal{Y}_{n-1}]$ are obtained. We will discuss each of these quantities individually.

Since the additive receiver noise is Gaussian, it is clear from the signal model (5) that $y(n)$ conditioned on $\mathbf{d}(n)$ is Gaussian with mean $\mathbf{h}_n^\top \mathbf{d}(n)$ and variance σ^2 . Hence $p[y(n) | \mathbf{d}(n)]$ is easily obtained.

Next, we note that

$$p[y(n) | \mathcal{Y}_{n-1}] = \sum_{\mathbf{d}(n)} P[\mathbf{d}(n) | \mathcal{Y}_{n-1}] \cdot p[y(n) | \mathbf{d}(n)] \quad (17)$$

and so our problem now reduces to finding the two conditional probability functions on the RHS of (17), since they appear in (16) as well.

If the instant n is not a symbol boundary for any user, $P[\mathbf{d}(n) | \mathcal{Y}_{n-1}]$ in (15) is given by

$$P[\mathbf{d}(n) | \mathcal{Y}_{n-1}] = P[\mathbf{d}(n-1) | \mathcal{Y}_{n-1}]. \quad (18)$$

However, at a symbol boundary, $\mathbf{d}(n) = \Phi_n \mathbf{d}(n-1) + \mathbf{w}(n)$ as shown in (7), where $\Phi_n \neq \mathbf{I}$ and $\mathbf{w}(n) \neq \mathbf{0}$. Then, clearly, we have

$$P[\mathbf{d}(n) | \mathbf{d}(n-1)] = P_w[\mathbf{d}(n) - \Phi_n \mathbf{d}(n-1)] \quad (19)$$

where $P_w(\mathbf{w})$ is the pmf of $\mathbf{w}(n)$ given by

$$P_w \left(\mathbf{w} = \begin{pmatrix} \mathbf{0} \\ \alpha_m \end{pmatrix} \right) = \frac{1}{M}$$

and $\alpha_m = \exp(j2\pi m/M)$, $m = 0, \dots, M-1$ for M -PSK modulation. Substituting (19) into (15) gives us

$$P[\mathbf{d}(n) | \mathcal{Y}_{n-1}] = \frac{1}{M} \sum_{\mathbf{d}(n-1) \in \mathcal{D}} P[\mathbf{d}(n-1) | \mathcal{Y}_{n-1}] \quad (20)$$

where \mathcal{D} is the set of all M vectors $\mathbf{d}(n-1)$ which can result in $\mathbf{d}(n)$. To understand this, recall that $\mathbf{d}(n)$ and $\mathbf{d}(n-1)$ have all but one element in common. Specifying $\mathbf{d}(n)$ therefore fixes all but one component of $\mathbf{d}(n-1)$, which is a discrete random variable that may take one of M values with equal probability.

The optimal MMSE estimate of the symbol $d_k(i)$ in the vector $\mathbf{d}(n)$ is given by

$$\hat{d}_k(i) = \sum_{m=1}^M \sum_{\mathbf{d}(n), d_k(i)=\alpha_m} \alpha_m P[\mathbf{d}(n) | \mathcal{Y}_n]. \quad (21)$$

Alternatively, the MAP estimate of the vector $\mathbf{d}(n)$ can be obtained by maximizing $P[\mathbf{d}(n) | \mathcal{Y}_n]$.

In either case, the complexity is on the order of $M^{(N_d+1)K}$, just as in the maximum-likelihood detector, and the MAP and optimal MMSE detectors are therefore impractical. Nonetheless, the algorithm proposed here is novel in that it is a chip-rate recursive optimal detector.

B. Nonlinear Kalman-Type Detectors

As the optimal MMSE detector has a complexity that is exponential in the number of users K , we hereby propose three suboptimal nonlinear Kalman-type detectors, each of which is formed by a linear Kalman detector and a nonlinear decision-feedback section that is invoked at symbol boundaries.

The proposed class of detection algorithms consists of two distinct steps. When we are not at any symbol boundary, we implement the linear Kalman detector because the state noise $\mathbf{w}(n)$ is nonexistent (and hence can be assumed Gaussian). But at every symbol boundary, an additional processing step is added in order to account for the non-Gaussianity of $\mathbf{w}(n)$ then. At the k th user's symbol boundary, we insert into the received signal sequence $y(n)$ either a hard decision or soft decision on the symbol $d_k(i - N_d)$, the symbol about to be shifted out of the state vector $\mathbf{d}(n)$. This creates an "additional" observation [8], [9] $y_a(n-1)$, so that the observation sequence becomes $\{\dots, y(n-2), y(n-1), y_a(n-1), y(n), \dots\}$.

Assuming that $y_a(n-1) = d_k(i - N_d)$, we can write

$$y_a(n-1) = \mathbf{h}_{n-1,a}^\top \mathbf{d}(n-1) \quad (22)$$

where $\mathbf{h}_{n-1,a}^\top = [\underbrace{0, \dots, 0}_{N_d K + k - 1}, \underbrace{1, 0, \dots, 0}_{K - k - 1}]$, and the nonzero element "1" is in the $(N_d K + k)$ th position, and use it as the observation equation for $y_a(n-1)$. An improved soft estimate of $\mathbf{d}(n-1)$, denoted $\hat{\mathbf{d}}_a(n-1)$, will be generated and the linear Kalman filter updates will continue with it as the filtered state estimate of $\mathbf{d}(n-1)$. In (22) and the rest of the paper, the subscript a denotes variables associated with the additional observation.

Based on the additional observation concept, we will develop two types of nonlinear Kalman detectors. The first is an HD feedback Kalman detector, while the second contains two SD feedback Kalman detectors.

1) *HD Feedback Kalman Detector*: The principle is that we make a hard decision on $\hat{d}_k(i - N_d)$, which comes from the linear Kalman filter, and assign it to $y_a(n-1)$. The operation is $y_a(n-1) = H(\hat{d}_k(i - N_d))$, where for M -PSK $H(x) =$

$e^{j2\pi\hat{m}/M}$ and $\hat{m} = \operatorname{argmin}_m |x - e^{j2\pi m/M}|^2$. For binary phase-shift keying (BPSK), $H(x) = \operatorname{sgn}[\operatorname{Re}(x)]$. Then, using (22) as the observation equation, and treating $\hat{\mathbf{d}}(n-1)$ as the predicted state estimate, the Kalman filter update equations are as follows:

$$\mathbf{k}_{n-1,a} = \frac{\mathbf{P}_{n-1}^+ \mathbf{h}_{n-1,a}}{\mathbf{h}_{n-1,a}^\top \mathbf{P}_{n-1}^+ \mathbf{h}_{n-1,a}} \quad (23)$$

$$\mathbf{P}_{n-1,a} = (\mathbf{I} - \mathbf{k}_{n-1,a} \mathbf{h}_{n-1,a}^\top) \mathbf{P}_{n-1}^+ \quad (24)$$

$$\hat{\mathbf{d}}_a(n-1) = \hat{\mathbf{d}}(n-1) + \mathbf{k}_{n-1,a} \cdot \left[y_a(n-1) - \mathbf{h}_{n-1,a}^\top \hat{\mathbf{d}}(n-1) \right]. \quad (25)$$

Finally, we set $\hat{\mathbf{d}}(n-1) = \hat{\mathbf{d}}_a(n-1)$ and $\mathbf{P}_{n-1}^+ = \mathbf{P}_{n-1,a}$ and continue with the linear Kalman detector updates. At the symbol boundaries, we are effectively feeding back hard decisions to improve detection performance, so that the detector can be considered an HD feedback detector. From (25), it is notable that the symbol decision is $\hat{d}_{k,a}(i-N_d) = y_a(n-1) = H(\hat{d}_k(i-N_d))$, and therefore the feedback operation does not impact the detection of $d_k(i-N_d)$. However, it will improve the detection performance of all future symbols.

2) *SD Feedback Kalman Detector I*: In this section and the next, we will develop two different SD feedback Kalman detectors. For the first SD detector, we assign to $y_a(n-1)$ the value

$$y_a(n-1) = \bar{\alpha}(n-1) = \sum_{m=1}^M \alpha_m g_{n-1}^{(m)} \quad (26)$$

where $g_{n-1}^{(m)} = \hat{P}(d_k(i-N_d) = \alpha_m | \mathcal{Y}_{n-1})$ is the estimated probability⁵ that $d_k(i-N_d) = \alpha_m$, given observations \mathcal{Y}_{n-1} .

To find the M values of $g_{n-1}^{(m)}$ needed to form $y_a(n-1)$, we assume that $\mathbf{d}(n-1)$, conditioned on \mathcal{Y}_{n-1} , is a complex Gaussian vector with mean $\hat{\mathbf{d}}(n-1)$ (the output of the Kalman filter) and covariance matrix \mathbf{P}_{n-1}^+ (also obtained from the Kalman filter). Then, the conditional pdf for the desired component $d_k(i-N_d)$, evaluated at α_m , is

$$\begin{aligned} \hat{p}(\alpha_m) &= \hat{p}(d_k(i-N_d) = \alpha_m | \mathcal{Y}_{n-1}) \\ &= \frac{1}{2\pi\sigma_d^2} \exp\left(-\frac{1}{2} \frac{|\alpha_m - \hat{d}_k(i-N_d)|^2}{\sigma_d^2}\right) \end{aligned} \quad (27)$$

where $\sigma_d^2 = \mathbf{h}_{n-1,a}^\top \mathbf{P}_{n-1}^+ \mathbf{h}_{n-1,a}$.

The probabilities $g_{n-1}^{(m)}$ are then obtained by normalizing $\hat{p}(\alpha_m)$ over all m , i.e.,

$$g_{n-1}^{(m)} = \frac{\hat{p}(\alpha_m)}{\sum_{m=1}^M \hat{p}(\alpha_m)}. \quad (28)$$

If $\mathbf{d}(n-1)$ were in fact Gaussian, $\hat{\mathbf{d}}(n-1)$ and \mathbf{P}_{n-1}^+ will indeed be its conditional mean and covariance, respectively. Then, of course, the linear Kalman filter will deliver the CM (and hence optimal MMSE) estimates.

The Kalman filter update equations (23)–(25) are now executed, with $y_a(n-1)$ computed from (26). For BPSK ($M = 2$), it may be shown [8], [9] that

⁵Since some probability functions introduced in subsequent sections of the paper are obtained approximately using the Gaussian assumption, we use \hat{p} or \hat{P} to denote them.

$y_a(n-1) = \tanh(\operatorname{Re}(\mathbf{h}_{n-1,a}^\top \hat{\mathbf{d}}(n-1))/\sigma_d^2)$, where $\tanh(\cdot)$ is the hyperbolic tangent function. We extract $\hat{d}_k(i-N_d)$ from $\hat{\mathbf{d}}_a(n-1)$ as the detector output and then continue the linear Kalman filter updates after replacing $\hat{\mathbf{d}}(n-1)$ with $\hat{\mathbf{d}}_a(n-1)$. The soft symbol output is $\hat{d}_{k,a}(i-N_d) = y_a(n-1)$. The resulting detector is called the SD Kalman detector I.

3) *SD Feedback Kalman Detector II*: The second SD Kalman detector is obtained by noting that the desired value of $\hat{\mathbf{d}}_a(n-1)$ is $E[\mathbf{d}(n-1) | \mathcal{Y}_{n-1}]$, and that of $\mathbf{P}_{n-1,a}$ is

$$\begin{aligned} \mathbf{P}_{n-1,a} &= E \left\{ [\mathbf{d}(n-1) - \hat{\mathbf{d}}_a(n-1)][\mathbf{d}^H(n-1) \right. \\ &\quad \left. - \hat{\mathbf{d}}_a^H(n-1)] | \mathcal{Y}_{n-1} \right\}. \end{aligned} \quad (29)$$

Therefore, let us assume that $\mathbf{d}(n-1)$ conditioned on \mathcal{Y}_{n-1} is continuously distributed with mean $\hat{\mathbf{d}}_a(n-1)$ and covariance matrix $\mathbf{P}_{n-1,a}$, find an estimate for $p[\mathbf{d}(n-1) | \mathcal{Y}_{n-1}]$ using the information we have available, and obtain $\hat{\mathbf{d}}_a(n-1)$ and $\mathbf{P}_{n-1,a}$ from this estimated pdf.

We start with the Bayesian factorization

$$\begin{aligned} \hat{p}(\mathbf{d}(n-1) | \mathcal{Y}_{n-1}) \\ = \sum_{m=1}^M g_{n-1}^{(m)} \hat{p}(\mathbf{d}(n-1) | d_k(i-N_d) = \alpha_m, \mathcal{Y}_{n-1}). \end{aligned} \quad (30)$$

To evaluate the conditional pdf on the RHS, we assume that $\mathbf{d}(n-1)$ conditioned on $d_k(i-N_d) = \alpha_m$ and \mathcal{Y}_{n-1} is Gaussian, so that its mean and covariance may, respectively, be computed using the Kalman filter updates

$$\begin{aligned} \hat{\mathbf{d}}^{(m)}(n-1) &= \hat{\mathbf{d}}(n-1) + \frac{\mathbf{P}_{n-1}^+ \mathbf{h}_{n-1,a}}{\sigma_d^2} \\ &\quad \times \left(\alpha_m - \mathbf{h}_{n-1,a}^\top \hat{\mathbf{d}}(n-1) \right) \end{aligned} \quad (31)$$

$$\mathbf{P}_{n-1}^{(m)} = \mathbf{P}_{n-1}^+ - \frac{\mathbf{P}_{n-1}^+ \mathbf{h}_{n-1,a} \mathbf{h}_{n-1,a}^\top \mathbf{P}_{n-1}^+}{\sigma_d^2}. \quad (32)$$

These are obtained from (23)–(25) through the substitution $y_a(n-1) = d_k(i-N_d) = \alpha_m$. It is notable that $\mathbf{P}_{n-1}^{(m)}$ is independent of m and equivalent to (24).

In theory, we can now compute $\hat{\mathbf{d}}_a(n-1) = \sum_{\mathbf{d}(n-1)} \mathbf{d}(n-1) \hat{p}(\mathbf{d}(n-1) | \mathcal{Y}_{n-1})$, but this will entail a complexity identical to the optimal MMSE detector derived in Section III-A. Instead, we take the Laplace transform of both sides of (30) to obtain the moment generating function (MGF) of $\mathbf{d}(n-1)$ conditioned on \mathcal{Y}_{n-1}

$$\hat{C}_{n-1,a}(\mathbf{s}) = \sum_{m=1}^M g_{n-1}^{(m)} \hat{C}_{n-1}^{(m)}(\mathbf{s}) \quad (33)$$

$$\begin{aligned} &= \sum_{m=1}^M g_{n-1}^{(m)} \exp\left(\mathbf{s}^H \hat{\mathbf{d}}^{(m)}(n-1) + \mathbf{s}^H \mathbf{P}_{n-1}^{(m)} \mathbf{s}\right) \end{aligned} \quad (34)$$

where the second line comes from the Gaussian assumption.

By definition, the first- and second-order moments of a random vector are given by the first and second derivatives of its MGF evaluated at the origin, respectively. Therefore, we

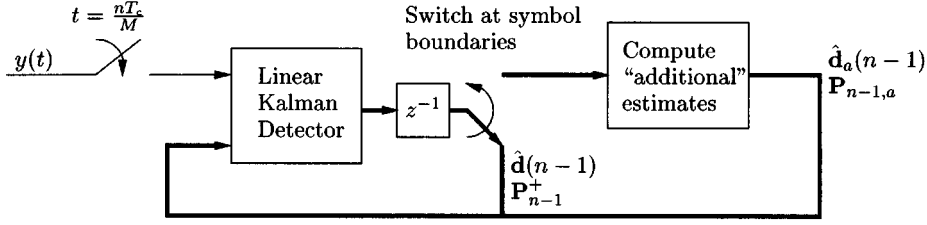


Fig. 3. Generic block diagram of the Kalman filter-based nonlinear detectors. z^{-1} denotes a one-sample delay.

may obtain expressions for $\hat{\mathbf{d}}_a(n-1)$ and $\mathbf{P}_{n-1,a}$ by differentiating (34) twice and setting $\mathbf{s} = \mathbf{0}$, and then substituting (31) and (32) to give the final expressions. These are

$$\begin{aligned} \hat{\mathbf{d}}_a(n-1) &= \sum_{m=1}^M g_{n-1}^{(m)} \hat{\mathbf{d}}^{(m)}(n-1) \\ &= \hat{\mathbf{d}}(n-1) + \mathbf{k}_{n-1,a} \left[\bar{\alpha}(n-1) - \mathbf{h}_{n-1,a}^\top \hat{\mathbf{d}}(n-1) \right] \end{aligned} \quad (35)$$

$$\begin{aligned} \mathbf{P}_{n-1,a} &= \sum_{m=1}^M g_{n-1}^{(m)} \left(\mathbf{P}_{n-1}^{(m)} + \hat{\mathbf{d}}^{(m)}(n-1) \hat{\mathbf{d}}^{(m),H}(n-1) \right. \\ &\quad \left. - \hat{\mathbf{d}}_a(n-1) \hat{\mathbf{d}}_a^H(n-1) \right) \\ &= \mathbf{P}_{n-1}^+ - \frac{\mathbf{P}_{n-1}^+ \mathbf{h}_{n-1,a} \mathbf{h}_{n-1,a}^\top \mathbf{P}_{n-1}^+}{\sigma_d^2} \\ &\quad \times \left(1 - \frac{1 - |\bar{\alpha}(n-1)|^2}{\sigma_d^2} \right). \end{aligned} \quad (36)$$

The SD Kalman detectors I and II differ only in the update of the covariance matrix \mathbf{P} , but their derivations are based on different philosophies as follows.

- 1) The SD detector I assumes that (22) is the correct observation equation to use, even though it is obvious that (22) is accurate only when correct hard decisions are fed back. It is however slightly simpler to implement than SD II, and as we show in simulations later, its performance is in between those of the HD and SD II detectors.
- 2) SD detector II uses the additional observation equation M times [see (31) and (32)], each time feeding back a different tentative hard decision α_m . The resulting state estimate vector and covariance matrix are then treated as the mean and covariance of $\mathbf{d}(n-1)$, conditioned on the desired transmitted symbol being α_m . To remove this conditioning, the MGF method is applied and we eventually arrive at (35) and (36).

Given that SD II uses a more rigorous approach, it will perform better, and its performance analysis is also easier to obtain, as will be seen later.

4) *Summary of the Kalman Filter-Based Nonlinear Detectors:* Fig. 3 is a block diagram applicable to the Kalman detectors of the last two sections. Basically, the analog baseband received signal is converted to a discrete-time sequence at M times the chip rate. The sequence $y(n)$ is then processed by the

linear Kalman detector of Section II-B, which outputs $\hat{\mathbf{d}}(n)$ and \mathbf{P}_n^+ at the sampling rate (M/T_c) . Outside the symbol boundaries, the linear detector outputs are fed back in order to generate the next set of estimates using (14). At a symbol boundary, we compute additional estimates $\hat{\mathbf{d}}_a(n-1)$ and \mathbf{P}_{n-1}^+ , which then replace $\mathbf{d}(n-1)$ and \mathbf{P}_{n-1}^+ , respectively, in (14).

C. Probability of Error Analysis

From the results of the previous sections, we can evaluate the symbol-error probability (SEP) of the proposed Kalman detectors. For a linear Kalman detector, it is known that $\mathbf{P}_n^+ = E(\varepsilon(n)\varepsilon^H(n) | \mathcal{Y}_n)$ in (13) is the covariance matrix of the filtered error vector $\varepsilon(n) = \hat{\mathbf{d}}(n) - \mathbf{d}(n)$. Thus the diagonal elements of \mathbf{P}_n^+ represents the MSE of the soft-decision statistics. For a symbol boundary n , let $a_k = N_d K + k$, then $\xi_k(i) = \mathbf{P}_{n-1}^+(a_k, a_k)$ (the a_k th diagonal element of \mathbf{P}_{n-1}^+) denotes the estimation MSE for the k th user with N_d symbols of detection delay.

For the linear MMSE detector, there is a relationship between the signal-to-interference-plus-noise ratio (SINR) γ and the residual MSE, given by [14, eq. (13)]. Using that result, the instantaneous SINR for the k th user in the i th symbol interval is given by

$$\gamma_k(i) = \frac{1 - \xi_k(i)}{\xi_k(i)}. \quad (37)$$

Since the proposed Kalman detector gives LMMSE estimates, and it is known that the residual interference and noise term at the output of an LMMSE detector is near-Gaussian [15], the instantaneous SEP for M -PSK is simply [16]

$$P_k^M(i) = \frac{1}{\pi} \int_0^{(M-1)\pi/M} \exp\left(-\frac{g_{\text{psk}} \gamma_k(i)}{\sin^2 \theta}\right) d\theta \quad (38)$$

where $g_{\text{psk}} = \sin^2(\pi/M)$. For BPSK, the bit-error probability (BEP) is $Q(\sqrt{\gamma_k(i)})$, where $Q(x) = \int_x^\infty 1/\sqrt{2\pi} e^{-0.5t^2} dt$ is the complementary unit Gaussian cumulative distribution function. Averaging (38) over all $\gamma_k(i)$, which may in practice be computed by averaging over a sufficiently large number of symbol intervals, gives the unconditional SEP for user k .

Equations (37) and (38) are especially useful for computing the SEP for random-code and/or fading CDMA channels, since the SEP for any symbol interval can be computed online by $\xi_k(i)$ given in \mathbf{P}_{n-1}^+ . This is significantly more efficient than computing the equivalent matrix filter (see [17] for some idea of how this is done) \mathbf{F}_{mse} for every symbol interval, and then computing the SEP.

Of the nonlinear detectors, only the SD II's performance can be analyzed in an analogous fashion. This is because of the following. 1) The HD detector suffers from decision-feedback errors, which are not reflected in the covariance estimates, which therefore tend to under-estimate the actual covariance. 2) The SD I detector updates the covariance estimate in a simplified but less accurate manner than does the SD II. For the SD II detector, the following method works well.

We note that from $\mathbf{P}_{n-1,a}$ given in (36), we can obtain the MSE after the decision-feedback operation as $\xi_{k,a}(i) = \mathbf{P}_{n-1,a}(a_k, a_k)$. If we assume that $\xi_{k,a}(i)$ is Gaussian, then $\xi_{k,a}(i)$ can be used to compute the instantaneous SINR, as in (37), from which the BEP can be obtained.

Another method for computing the BEP of the SD II detector, based on estimated probability distributions, is provided in the Appendix.

IV. COMPLEXITY

The complexity of the proposed detectors is studied in this section. It will be shown that $O(K^2)$ multiplications per detected symbol are required for each of the detectors, and this compares favorably to other multiuser detectors such as the linear decorrelator.

A. Useful Observations

Although the Kalman filter time-update equations may look intimidating and highly complex to implement, a closer inspection reveals that many of the matrices and vectors involved are sparse, and therefore the updates are less complex than they appear at first sight. The matrix Φ_n used in the linear Kalman detector, and the vector $\mathbf{h}_{n-1,a}$ in the nonlinear detector will be highlighted.

State Transition Matrix Φ_n In (11), we apparently need to multiply three square matrices together, when actually that update is not required except at symbol boundaries (since $\Phi_n = \mathbf{I}$). And then the form of Φ_n at symbol boundaries requires only a shifting of elements of \mathbf{P}_{n-1}^+ , as we now illustrate with

$$\Phi_n = \begin{bmatrix} 1 & 0 & 0 & 0 \\ 0 & 0 & 0 & 0 \\ 0 & 0 & 1 & 0 \\ 0 & 1 & 0 & 0 \end{bmatrix}$$

which will be the state transition matrix at the second user's symbol boundary, when $K = 2$ and $N_d = 1$.

In this case, it is easily shown that for $(\mathbf{P}_{n-1}^+)_{ij} = p_{ij}$, where $(\mathbf{A})_{ij}$ denotes the element of a matrix \mathbf{A} in the i th row and j th column, we have

$$\Phi_n \mathbf{P}_{n-1}^+ \Phi_n^\top = \begin{bmatrix} p_{11} & 0 & p_{13} & p_{12} \\ 0 & 0 & 0 & 0 \\ p_{31} & 0 & p_{33} & p_{32} \\ p_{21} & 0 & p_{23} & p_{22} \end{bmatrix}.$$

Therefore, no multiplications are needed.

Basically, $\Phi_n \mathbf{A}$ will rearrange the rows of \mathbf{A} , while $\mathbf{A} \Phi_n^\top$ rearranges the columns.

Additional Measurement Matrix $\mathbf{h}_{n-1,a}$ Because the vector $\mathbf{h}_{n-1,a}$ only has one nonzero element, $\mathbf{P}_{n-1}^+ \mathbf{h}_{n-1,a}$ is equal to one of the columns of \mathbf{P}_{n-1}^+ , and $\mathbf{h}_{n-1,a}^\top \mathbf{P}_{n-1}^+ \mathbf{h}_{n-1,a}$ is one of its diagonal elements. Therefore, (23) does not involve any multiplications in spite of its complicated form, and other operations needed in the nonlinear detectors are also simplified.

B. Linear Kalman Detector

For the linear detector, only multiplications and additions are needed and since the latter is known to be much less complex than the former, we will only look at the number of multiplications per user per symbol detected.

As explained previously, (11) requires no multiplications. Assuming that $N_d = 0^6$ and that a division is equivalent in operation count to a multiplication,⁷ (12) entails $K^2 + 2K$ multiplications. The update of \mathbf{P}_n^+ in (13) uses K^2 multiplications,⁸ while (14) takes $2K$ multiplications.

With T updates per symbol interval, the total multiplication count per symbol interval is $(2K^2 + 4K)T$. Given that exactly K symbols are detected in one symbol interval, the number of multiplications per symbol detected is $(2K + 4)T$, or $O(KT)$.⁹ Since T is of the order of K , the complexity can be said to be $O(K^2)$.

C. Nonlinear Detectors

All three nonlinear detectors differ from the linear Kalman detector only at the symbol boundaries, where they perform an extra update operation, as Fig. 3 clearly shows. Their complexity is therefore discussed in this section in terms of the *additional* complexity per detected symbol compared to the linear Kalman detector.

1) *HD Detector:* In (23), the numerator is one of the columns of \mathbf{P}_{n-1}^+ , while the denominator is one of its diagonal elements. Therefore, only K multiplications for the scalar division of the numerator by the denominator are required. We also note that (24) may be simplified by rewriting it as

$$\mathbf{P}_{n-1,a} = \mathbf{P}_{n-1}^+ - \frac{\mathbf{v}_{n-1} \mathbf{v}_{n-1}^H}{\sigma_d^2} \quad (39)$$

where $\mathbf{v}_{n-1} = \mathbf{P}_{n-1}^+ \mathbf{h}_{n-1,a}$ and σ_d^2 is defined below (27). Since any vector outer product $\mathbf{x} \mathbf{x}^H$ is Hermitian, only the diagonal and lower (or upper) triangular elements need to be found. Each of those elements is simply a product of two scalar quantities, and hence (39) requires $(K(K+1)/2) + K$ multiplications.

Finally, (25) requires K multiplications, and a slicing or HD operation is required to produce $y_a(n-1)$. In total, we therefore have a total of $(K(K+1)/2) + 3K$ additional multiplications

⁶The complexity is actually proportional to $(N_d + 1)^2$ for $N_d > 0$, but if the decoupled iterations for the Kalman-smoothing detector developed in [18] are employed, the complexity is proportional to $N_d + 1$.

⁷An assumption used throughout this section.

⁸Note that $\mathbf{P}_n^- \mathbf{h}_n$ can be precomputed for use in (12) and (13), and that \mathbf{P}_n^- is Hermitian.

⁹In [5] the operation count per symbol interval was given as $O(K^2 T)$, but since K symbols are detected therein, $O(KT)$ is a fairer reflection of the algorithm complexity.

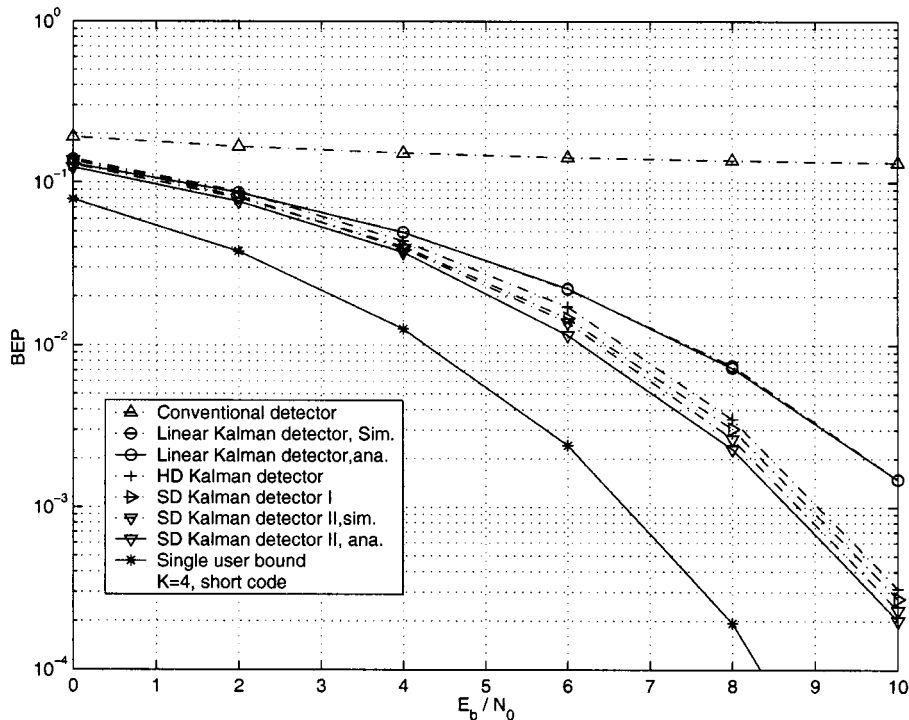


Fig. 4. BER performance of the linear and nonlinear Kalman detectors in an unfaded short-code CDMA channel.

and one HD operation per symbol detected, compared to the linear Kalman detector.

2) *SD Detector I*: This detector uses the same update equations as the HD detector, i.e., (23)–(25), but $y_a(n-1)$ is computed differently. Equation (27) entails one exponential operation, and three multiplications for the argument of the exponential function; (28) uses one multiplication. Since we need to compute M values of $g_{n-1}^{(m)}$, the total complexity of finding $y_a(n-1)$ from (26) is $5M$ multiplications and M exponential functions. We note that the normalizing factor $2\pi\sigma_d^2$ in (27) is not necessary, since only the relative values of $\hat{p}(\alpha_m)$, $m = 1, \dots, M$, are required to find $g_{n-1}^{(m)}$ using (28).

The additional complexity of the SD I detector compared to the linear Kalman detector is therefore $(K(K+1)/2) + 3K + 5M$ multiplications and M exponentials per symbol detected.

3) *SD Detector II*: This detector executes (23), (35), and (36) at each symbol boundary. Noting that $\bar{\alpha}(n-1)$ and $y_a(n-1)$ are equal by definition, we see that $5M$ multiplications and M exponential functions are needed to find $\bar{\alpha}(n-1)$. Equation (35) requires K multiplications, while (36) consumes $(K(K+1)/2) + K + 2$ multiplications.

The total additional complexity of the SD II detector is thus $(K(K+1)/2) + 3K + 5M + 2$ multiplications and M exponential functions.

V. SIMULATION RESULTS

In this section, we give some simulation results for the proposed linear and nonlinear Kalman detectors for BPSK modulation. We assume a symbol-asynchronous multiuser CDMA channel, where there are K active users and the spreading gain is $T = 8$. For unfaded or one-path Rayleigh fading channels,

we set $K = 4$ and the time delays for the four users are arbitrarily set to zero, two, four, and five chips, respectively. For simplicity, we have assumed that the time delays of all users are integer multiples of the chip interval, whereas it should be understood that our system model and proposed algorithms also apply to arbitrary time delays.

For two-path Rayleigh fading channels ($L = 2$), we have $K = 3$ and the time delays are $[\tau_{11}, \tau_{12}, \tau_{21}, \dots, \tau_{32}] = [0, 3, 1, 4, 2, 6]$ chips. For convenience, we assume that every user has equal power in each receiving path and the symbol energy is normalized to one, i.e., $E(|c_{kl}(i)|^2) = 1/L$ for all k, l . In all the simulations, we set the detection delay $N_d = 3$ and each curve gives the averaged BER for the K users.

Figs. 4 and 5 give the BER curves for the linear and nonlinear Kalman detectors, where the curves in Figs. 4 and 5 are for unfaded short-code and long-code CDMA channels, respectively. The short codes are randomly generated (“coin-flip”) bipolar sequences. For comparison purposes, BER curves for the conventional matched filter detector and the single-user bound are also plotted.

In these two and the following figures, the analytical BER curves for the linear Kalman detector and SD detector II are computed using (37) and (38) and averaged over all the symbols. It is observed that our analysis fits the simulations very well. The BER values were also computed by using the method proposed in the Appendix, but the results were almost identical to those obtained by using (37) and (38), so we do not show them explicitly.

From the simulations, it is clear that the nonlinear detectors perform significantly better than the linear Kalman detector, and for a BER level of around 10^{-3} , a difference of nearly 2 dB is discernible. Among the nonlinear detectors, the SD II detector

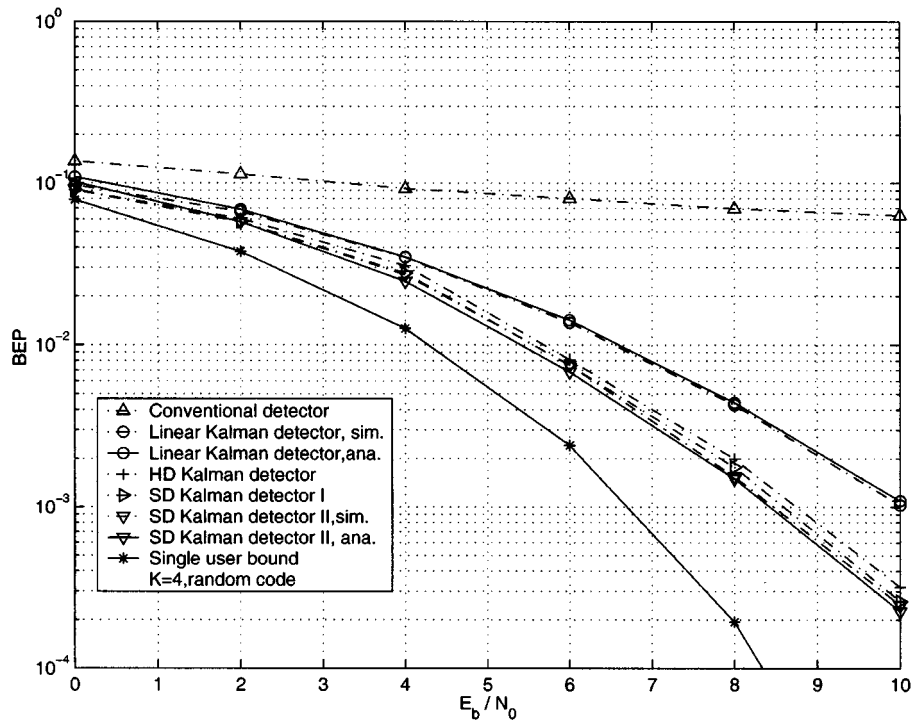


Fig. 5. BEP performance of the linear and nonlinear Kalman detectors in an unfaded random-code CDMA channel.

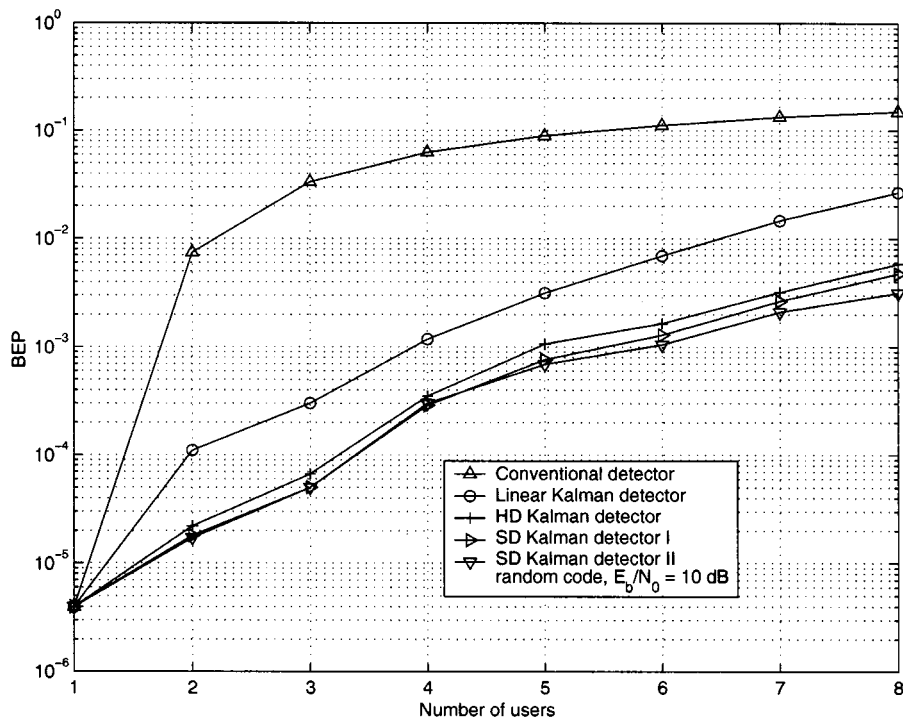


Fig. 6. BEP performance versus the number of users in an unfaded random-code CDMA channel.

performs slightly better than the SD I detector, which in turn does slightly better than the HD detector. It is notable that the complexity of the detector also decreases in that order.

Next, in Fig. 6, we plot BEP curves against the number of users K in a random-code unfaded CDMA channel. All the curves were obtained by simulations. As K increases, the BEP of the conventional detector degrades drastically, while

the degradation of the linear and nonlinear Kalman detectors is more graceful. Their BEP curves are of course always significantly lower than those of the conventional detector.

For simulation of a Rayleigh fading channel, we assume that the channel is constant within a symbol interval, but can be modeled as a first-order Markov process at the symbol rate. In other words, if $c_{kl}(i)$, $k \in [1, \dots, K]$, $l \in [1, \dots, L]$ denotes the com-

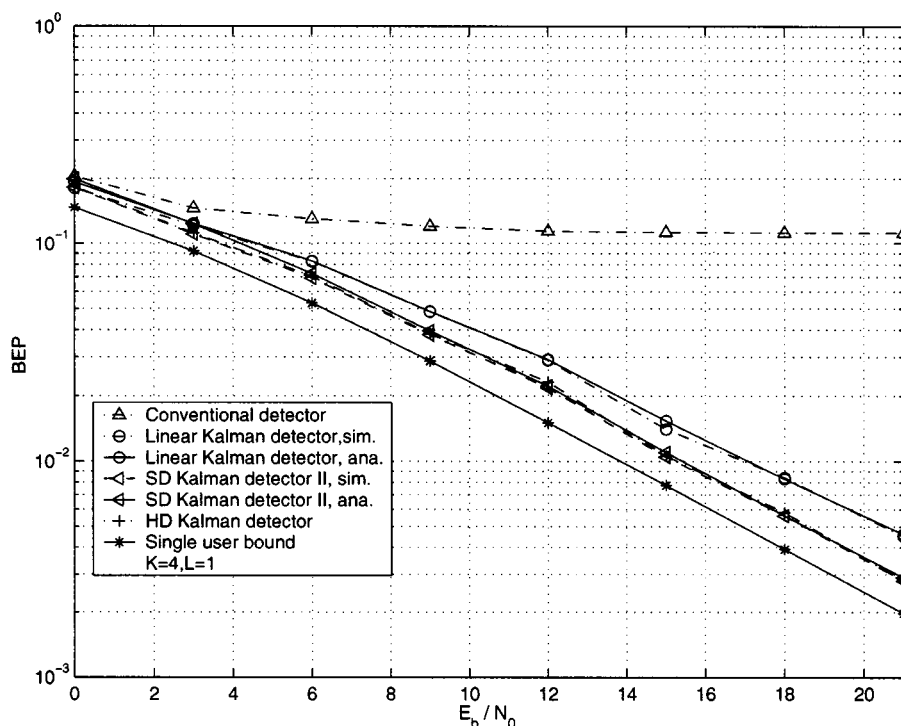


Fig. 7. BEP performance of the linear and nonlinear Kalman detectors in a single-path Rayleigh faded short-code CDMA channel.

plex attenuation of the l th path for the k th user in the i th symbol interval

$$c_{kl}(i) = \rho_{kl}c_{kl}(i-1) + \sqrt{1 - \rho_{kl}}v_{kl}(i) \quad (40)$$

where $v_{kl}(i)$ is a complex white Gaussian noise sequence with variance $1/L$, and $\rho_{kl} = E[c_{kl}^*(i-1)c_{kl}(i)]/E[c_{kl}^*(i)c_{kl}(i)]$ is the fading correlation coefficient which we set to $\rho = 0.995$ for all k and l .

It is known that ρ depends on the fading power density spectrum and the Doppler fading bandwidth B_d . For example, $\rho = J_0(2\pi B_d T_s)$ for Jake's land mobile communications fading spectrum and $\rho = \exp(-(\pi B_d T_s)^2)$ for the Gaussian fading spectrum, where T_s is a symbol duration. A comparison of ρ versus $B_d T_s$ for different fading power density spectra was given in [19]. Since we assume coherent data modulation and that perfect channel estimates are available, the detector performance is expected to be insensitive to ρ_{kl} .

Fig. 7 plots the BEP curves for the linear and nonlinear Kalman detectors in a single-path Rayleigh fading channel, with $K = 4$. It is observed that the proposed nonlinear detectors still perform better than the linear Kalman detector.

Next we consider a two-path Rayleigh fading channel, where $K = 3$. To make a fair comparison with the linear Kalman detector proposed in [5], we introduce the same detection delay of $N_d = 3$ for that detector using the technique proposed in this paper, but it does post-detection combining. The resulting detector is called the multipath Kalman detector. Owing to the multipath, the conventional detector here is the RAKE receiver, while the single-user bound is obtained by setting $K = 1$ and implementing the linear Kalman detector.

The BEP curves are plotted in Fig. 8. The HD detector and the SD detector I perform close to the SD detector II, so their curves were not plotted. The detectors we propose perform considerably better than the multipath Kalman detector. The performance advantage of the nonlinear Kalman detectors over the linear version is clear.

VI. DISCUSSION

A. Multiple Users with the Same Symbol Timing

When a number of users (say P) have the same symbol timing, for instance, on the synchronous downlink of a cellular system, there are two possible ways to tackle the problem as follows.

- Insert P additional observations, one for each user. The soft estimate vector $\hat{\mathbf{d}}_a(n-1)$ will thus be updated P times.
- Insert one vector additional observation, and so update $\hat{\mathbf{d}}_a(n-1)$ only once, but with a more complex update equation.

Which method yields better results remains to be seen and is the subject of current investigations.

B. Iterative Detection for Coded CDMA

There has been a lot of recent interest in iterative or "turbo" detection in coded CDMA systems (e.g., [20], [21]). In such turbo multiuser detectors, *a posteriori* probabilities (APPs) of the coded symbols transmitted have to be updated and passed between the component decoders. The inner decoder in this case is a multiuser detector capable of accepting and updating APPs. The SD detectors proposed in this paper can be easily adapted to perform this function in the following manner.

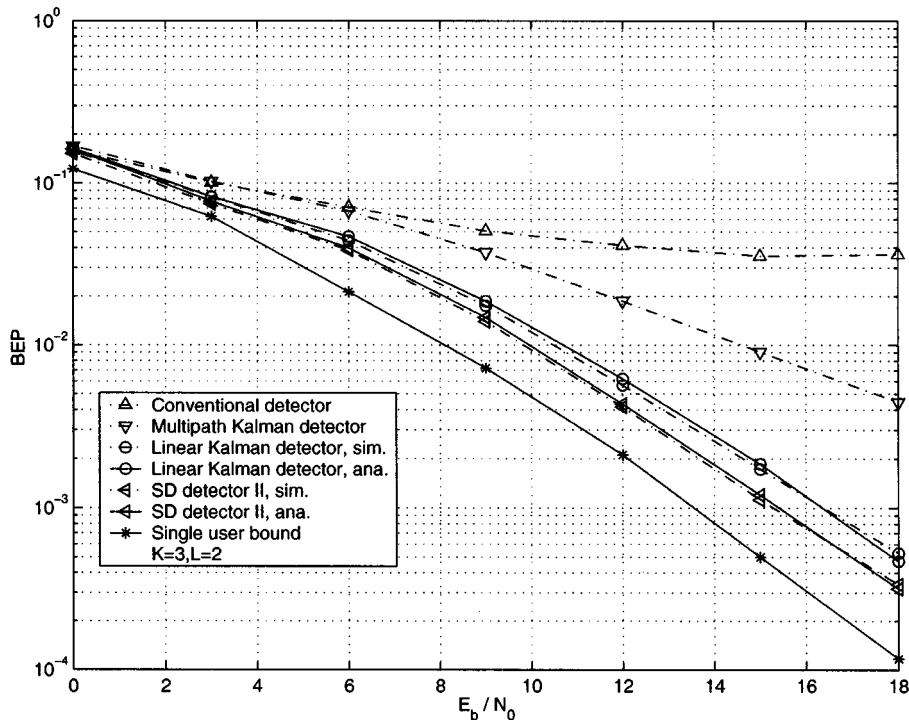


Fig. 8. BEP performance of the linear and nonlinear Kalman detectors in a two-path Rayleigh faded short-code CDMA channel.

- Given the APPs $g_{n-1}^{(m)}$, and hence $\bar{\alpha}(n-1)$, from the outer decoder, compute $\hat{\mathbf{d}}_a(n-1)$ using either the SD I or SD II algorithms.
- Extract the soft estimate of the desired symbol $d_k(i-N_d)$ from $\hat{\mathbf{d}}_a(n-1)$, and hence update the APPs $g_{n-1}^{(m)}$ with (27) and (28).

Given that the proposed algorithms are explicitly designed for asynchronous, multipath channels in which long codes are used, and generate APPs as a by-product, they may turn out to be more suited to iterative CDMA detection in practical systems than most other multiuser detectors.

C. Characteristics of Chip-Rate Kalman Multiuser Detector

Apart from being novel (and interesting because of that), the chip-rate Kalman filter approach to multiuser detection has a number of key practical and theoretical features, such as the following.

- 1) *Infinite memory*—the recursive nature of the Kalman filter means that it automatically makes use of all past information (see [17]) in forming an MMSE detector.
- 2) *Nonzero asymptotic multiuser efficiency*—in linear multiuser detection it is usually assumed that for asynchronous systems, code-matched filter outputs with windowing can be used [22]. However, this approach can lead to zero near-far resistance if the windowing method ignores the symbols at the edges of the window (for instance in order to create a square code-correlation matrix \mathbf{R} for decorrelation). The chip-rate approach on the other hand never has this problem because it accounts for all symbols directly contributing to the received signal *at all times*.

Both these points translate into better performance in practice.

VII. CONCLUSION

In this paper, we discussed an extension of the chip-rate Kalman detector of [5] to allow for arbitrary detection delays, derived a recursive algorithm for optimal nonlinear MMSE detection, and described several suboptimal nonlinear Kalman detectors based on the concept of additional observations [8], [9]. These algorithms are suited to long-code CDMA systems, and do not require matrix inversions although processing requirements are still substantial given that they operate at chip rate. Two semianalytic methods, which are far less complex than a method requiring the calculation of an equivalent matrix filter, for computing the average error probability in fading or nonfading channels were also presented and discussed. These methods can be used with averaging over many symbols to derive the unconditional error probability in long-code systems and/or multipath fading channels. Finally, we observed through simulations that the nonlinear Kalman detectors always performed better than the linear one, and that multipath combining before MMSE detection (pre-detection combining) is a superior technique to post-detection combining.

APPENDIX ALTERNATIVE BEP COMPUTATION METHOD FOR THE SD II DETECTOR

In this section, we will discuss another semianalytical approach to deriving the probability of error for the SD II detector, using our ability to approximately determine the APP $g_{n-1}^{(m)}$. In the rest of this section, we write $d_k(i-N_d)$ and $\hat{d}_k(i-N_d)$ (the output of the linear Kalman filter) as d and \hat{d} , respectively, for ease of notation.

We start by considering the case of BPSK, and then extending it to M -PSK. Assuming equiprobable transmitted bits, the BEP of user k is

$$P_{2,b} = \frac{1}{2}P(\hat{d} < 0 | d = 1) + \frac{1}{2}P(\hat{d} > 0 | d = -1). \quad (41)$$

Now, consider one of the conditional probabilities on the RHS (the other one is handled in exactly the same fashion).

$$\begin{aligned} P(\hat{d} > 0 | d = -1) &= \frac{P(\hat{d} > 0, d = -1)}{p(d = -1)} \\ &= 2P(\hat{d} > 0, d = -1). \end{aligned} \quad (42)$$

A simple application of Bayes' rule yields

$$P(\hat{d} > 0, d = -1) = \int_0^\infty P(d = -1 | \hat{d})p(\hat{d})d\hat{d} \quad (43)$$

$$\approx \frac{1}{N_1} \sum_{\hat{d} > 0} P(d = -1 | \hat{d}) \quad (44)$$

where N_1 is the number of terms in the summation, and $P(d = -1 | \hat{d})$ is obtained from (28). We should point out here that the assumption that \hat{d} is a sufficient statistic for the detection of d , given observations \mathcal{Y}_{n-1} , was implicitly made in (27). With this assumption, $g_{n-1}^{(m)} = \hat{P}(d = \alpha_m | \mathcal{Y}_{n-1})$ becomes equivalent to $\hat{P}(d = \alpha_m | \hat{d})$.

Combining (41), (42) and (44), the unconditional BEP for BPSK can be expressed as

$$P_{2,b} = P(\hat{d} < 0, d = 1) + P(\hat{d} > 0, d = -1) \quad (45)$$

$$\approx \frac{1}{N_1} \sum_{\hat{d} > 0} P(d = -1 | \hat{d}) + \frac{1}{N_2} \sum_{\hat{d} < 0} P(d = 1 | \hat{d}) \quad (46)$$

where N_1 and N_2 denote the number of symbols within the averaging window for which \hat{d} is positive and negative, respectively.

Another way to compute the average BEP for BPSK is given here. From (26), $\bar{\alpha} = P(d = 1 | \hat{d}) - P(d = -1 | \hat{d})$. Because of our Gaussian assumption, $P(d = 1 | \hat{d})$ is always smaller than $P(d = -1 | \hat{d})$ when $\hat{d} < 0$. The converse is also true. Therefore, the absolute value of $\bar{\alpha}$ can be represented as

$$|\bar{\alpha}| = \begin{cases} P(d = 1 | \hat{d}) - P(d = -1 | \hat{d}), & \text{if } \hat{d} > 0 \\ P(d = -1 | \hat{d}) - P(d = 1 | \hat{d}), & \text{if } \hat{d} < 0 \end{cases} \quad (47)$$

$$\begin{aligned} &= \begin{cases} 1 - 2P(d = -1 | \hat{d}), & \text{if } \hat{d} > 0 \\ 1 - 2P(d = 1 | \hat{d}), & \text{if } \hat{d} < 0 \end{cases} \\ \Rightarrow \frac{1 - |\bar{\alpha}|}{2} &= \begin{cases} P(d = -1 | \hat{d}), & \text{if } \hat{d} > 0 \\ P(d = 1 | \hat{d}), & \text{if } \hat{d} < 0 \end{cases} \end{aligned} \quad (48)$$

From the last equation, it should be clear that the expression (46) may be obtained by averaging $1/2(1 - |\bar{\alpha}|)$ over a large block of symbols, which therefore yields the BEP. This equality was used in [8] to compute the BEP, but its derivation was not described.

Now we extend the analysis to the M -PSK case. For SEP and BEP evaluation, we need to know the conditional probability $P(H(\hat{d}) = \alpha_m | d = \alpha_0 = 1)$, for $m = 0, 1, \dots, M-1$. Using (27) and (28) and averaging over a long symbol stream, we can compute the conditional probability $P(d = \alpha_m | H(\hat{d}) = \alpha_0)$ for $m = 0, 1, \dots, M-1$. Again, we have the equalities that $P(H(\hat{d}) = \alpha_m) = P(d = \alpha_m) = 1/M$ for all m , and

$$P(d = \alpha_0 | H(\hat{d}) = \alpha_m) = P(H(\hat{d}) = \alpha_m | d = \alpha_0). \quad (49)$$

The SEP and BEP can be computed easily by using (49). For example, for QPSK we have the SEP as

$$P_{4,s} = 1 - P(d = \alpha_0 | H(\hat{d}) = \alpha_0). \quad (50)$$

For Gray-coded QPSK the BEP is

$$\begin{aligned} P_{4,b} &= \frac{1}{2}(P(d = \alpha_1 | H(\hat{d}) = \alpha_0) \\ &+ 2P(d = \alpha_2 | H(\hat{d}) = \alpha_0) \\ &+ P(d = \alpha_3 | H(\hat{d}) = \alpha_0)), \end{aligned} \quad (51)$$

ACKNOWLEDGMENT

The authors would like to acknowledge useful discussions with Prof K. Q. T. Zhang of Ryerson Polytechnic University, Toronto, ON, Canada, in the initial stages of writing up this work.

REFERENCES

- [1] S. Verdú, *Multuser Detection*, Cambridge, U.K.: Cambridge Univ. Press, 1998.
- [2] Z. Xie, R. T. Short, and C. K. Rushforth, "A family of suboptimum detectors for coherent multiuser communications," *IEEE J. Select. Areas Commun.*, vol. 8, pp. 683–690, May 1990.
- [3] T. J. Lim and S. Roy, "Adaptive filters in multiuser CDMA detection," *Baltzer Wireless Networks*, vol. 4, no. 4, pp. 307–318, 1998.
- [4] G. Woodward and B. S. Vucetic, "Adaptive detection for DS-CDMA," *Proc. IEEE*, vol. 86, pp. 1413–1434, July 1998.
- [5] T. J. Lim, L. K. Rasmussen, and H. Sugimoto, "An adaptive asynchronous multiuser CDMA detector based on the Kalman filter," *IEEE J. Select. Areas Commun.*, vol. 16, pp. 1711–1722, Dec. 1998.
- [6] D. S. Chen and S. Roy, "An adaptive multiuser receiver for CDMA systems," *IEEE J. Select. Areas Commun.*, vol. 12, pp. 808–816, June 1994.
- [7] T. J. Lim, L. K. Rasmussen, and H. Sugimoto, "A Multiuser Code Division Multiple Access Receiver Based on Recursive Estimation," Patent Application 9703052-2, Aug. 1997.
- [8] J. Thielecke, "A state-space multiuser detector for CDMA systems," *Proc. IEEE Int. Conf. Communications (ICC'93)*, vol. 3, pp. 1762–1767, May 1993.
- [9] —, "A soft-decision state-space equalizer for FIR channels," *IEEE Trans. Commun.*, vol. 45, pp. 1208–1217, Oct. 1997.
- [10] H. C. Huang and S. Schwartz, "A comparative analysis of linear multiuser detectors for fading multipath channels," in *Proc. GLOBECOM*, San Francisco, CA, Dec. 1994, pp. 11–15.
- [11] H. C. Huang and S. Verdú, "Linear differentially coherent multiuser detection for multipath channels," *Wireless Pers. Commun.*, vol. 6, pp. 113–136, 1998.
- [12] J. M. Mendel, *Lessons in Estimation Theory for Signal Processing, Communications, and Control*. Englewood Cliffs, NJ: Prentice-Hall, 1995.
- [13] H. Stark and J. W. Woods, *Probability, Random Processes, and Estimation Theory for Engineers*, 2nd ed. Englewood Cliffs, NJ: Prentice-Hall, 1994.

- [14] U. Madhow and M. L. Honig, "MMSE interference suppression for direct-sequence spread-spectrum CDMA," *IEEE Trans. Commun.*, vol. 42, pp. 3178–3188, Dec. 1994.
- [15] H. V. Poor and S. Verdú, "Probability of error in MMSE multiuser detection," *IEEE Trans. Inform. Theory*, vol. 43, pp. 858–871, May 1997.
- [16] M. K. Simon and M.-S. Alouini, "A unified performance analysis of digital communication with dual selective combining diversity over correlated Rayleigh and Nakagami-m fading channels," *IEEE Trans. Commun.*, vol. 47, pp. 33–43, Jan. 1999.
- [17] T. J. Lim and Y. Ma, "The Kalman filter as the optimal linear minimum mean squared error multiuser CDMA detector," *IEEE Trans. Inform. Theory*, vol. 46, pp. 2561–2566, Nov. 2000.
- [18] Y. Ma, "Diversity Reception in Fading Channels and CDMA Multiuser Detection," Ph.D. dissertation, Nat. Univ. Singapore, 2000.
- [19] P. Y. Kam, "Bit error probabilities of MDPSK over the nonselective Rayleigh fading channel with diversity reception," *IEEE Trans. Commun.*, vol. 39, pp. 220–224, Feb. 1991.
- [20] M. C. Reed, C. B. Schlegel, P. D. Alexander, and J. A. Asenstorfer, "Iterative multiuser detection for CDMA with FEC: Near-single-user performance," *IEEE Trans. Commun.*, vol. 46, pp. 1693–1699, Dec. 1998.
- [21] X. Wang and H. V. Poor, "Iterative (turbo) soft interference cancellation and decoding for coded CDMA," *IEEE Trans. Commun.*, vol. 47, pp. 1046–1061, July 1999.
- [22] M. J. Juntti and B. Aazhang, "Finite memory-length linear multiuser detection for asynchronous CDMA communications," *IEEE Trans. Commun.*, vol. 45, pp. 611–622, May 1997.



Yao Ma (S'98–M'01) was born in Anhui, China, on November 6, 1971. He received the B.Eng. degree from Anhui University, the M.Sc. degree from University of Science and Technology of China (USTC), China, in 1993 and 1996, respectively, both in electrical engineering and information science, and the Ph.D. degree with the Electrical and Computer Engineering Department, National University of Singapore, in 2000. His Ph.D. dissertation was on performance analysis of diversity reception in fading channels and CDMA multiuser detection schemes.

He is currently in the Digital Communications Strategic Research Group at the Centre for Wireless Communications, Singapore. His research interests include performance analysis of wireless digital communications over general fading channels, interference cancellation in CDMA, and linear and nonlinear optimum filtering and its application in communications.



Teng Joon Lim (S'92–M'95) was born in Singapore on May 4, 1967. He received the B.Eng. degree (first-class honors) in electrical engineering from the National University of Singapore (NUS), in 1992, and the Ph.D. degree from the University of Cambridge, Cambridge, U.K., in early 1996 on a Cambridge Commonwealth Trust/British Telecom scholarship.

Since September 1995 to November 2000, he was with the Centre for Wireless Communications, Singapore, as a Senior Member of Technical Staff. In December 2000, he joined the Electrical and Computer Engineering Department of the University of Toronto, Toronto, ON, Canada, where he is currently an Assistant Professor. His research interests include multiuser detection, CDMA receiver design, turbo detection for coded CDMA, multicarrier modulation, and statistical signal processing applied to wireless communications.

Dr. Lim was the Digital Communications Strategic Research Group Leader, the Technical Program Chair for the IEEE Singapore International Conference on Communication Systems (ICCS 2000), an Adjunct Teaching Fellow at the NUS, and Secretary of the Singapore Chapter of the IEEE Communications Society.